Proton magnetic resonance spectroscopy and perfusion magnetic resonance imaging in the evaluation of musculoskeletal tumors*

Espectroscopia de prótons e perfusão por ressonância magnética na avaliação dos tumores do sistema musculoesquelético

Flávia Martins Costa[1], Evandro Miguelote Vianna[2], Rômulo Côrtes Domingues[2], Marcela Setti[3], Walter Meohas[4], José Francisco Rezende[4], Romeu Côrtes Domingues[5], Emerson Leandro Gasparetto[6]

Abstract **OBJECTIVE: To assess the role of proton magnetic resonance spectroscopy and dynamic contrast-enhanced magnetic resonance imaging in the differentiation between malignant and benign musculoskeletal tumors. MATERIALS AND METHODS: Fifty-five patients with musculoskeletal tumors (27 malignant and 28 benign) were studied. The examinations were performed in a 1.5 T magnetic resonance scanner with standard protocol, and single voxel proton magnetic resonance spectroscopy with 135 msec echo time. The dynamic contrast study was performed using T1-weighted gradient-echo sequence after intravenous gadolinium injection. Time-signal intensity curves and slope values were calculated. The statistical analysis was performed with the Levene's test, followed by a Student's *t*-test, besides the Pearson's chi-squared and Fischer's exact tests. RESULTS: Proton magnetic resonance spectroscopy sensitivity, specificity and accuracy were, respectively, 87.5%, 92.3% and 90.9% ($p < 0.0001$). Statistically significant difference was observed in the slope (%/min) between benign (mean, 27.5%/min) and malignant (mean, 110.9%/min) lesions ($p < 0.0001$). CONCLUSION: The time-intensity curve and slope values using dynamic-enhanced perfusion magnetic resonance imaging in association with the presence of choline peak demonstrated by single voxel magnetic resonance spectroscopy study are useful in the differentiation between malignant and benign musculoskeletal tumors.**

Keywords: Proton magnetic resonance spectroscopy; Perfusion magnetic resonance imaging; Magnetic resonance imaging.

Resumo **OBJETIVO: Avaliar a espectroscopia de prótons e o estudo dinâmico do contraste por ressonância magnética na diferenciação dos tumores musculoesqueléticos benignos e malignos. MATERIAIS E MÉTODOS: Foram estudados 55 pacientes com tumores musculoesqueléticos (27 malignos e 28 benignos). Os exames foram realizados em aparelho de ressonância magnética de 1.5 T com protocolo convencional e espectroscopia de prótons com TE de 135 ms. O estudo dinâmico do contraste foi adquirido pela sequência T1 gradiente-eco após a administração intravenosa de gadolínio. Curvas de intensidade de sinal *versus* tempo e valores de *slope* foram calculados. A análise estatística foi realizada pelo teste de Levene, seguido pelo teste *t* de Student, além dos testes qui-quadrado de Pearson e exato de Fischer. RESULTADOS: A sensibilidade, especificidade e acurácia da espectroscopia de prótons foram, respectivamente, de 87,5%, 92,3% e 90,9% ($p < 0,0001$). Além disso, houve significativa diferença entre o valor quantitativo da curva entre as lesões benignas (média de 27,5% por minuto) e malignas (média de 110,9% por minuto) ($p < 0,0001$). CONCLUSÃO: Os estudos quantitativo e qualitativo da análise dinâmica do contraste por ressonância magnética associados à presença do pico de colina são úteis na diferenciação dos tumores musculoesqueléticos em benignos e malignos.**

Unitermos: Espectroscopia de prótons; Perfusão; Imagem por ressonância magnética.

Costa FM, Vianna EM, Domingues RC, Setti M, Meohas W, Rezende JF, Domingues RC, Gasparetto EL. Proton magnetic resonance spectroscopy and perfusion magnetic resonance imaging in the evaluation of musculoskeletal tumors. Radiol Bras. 2009;42(4):215–223.

INTRODUCTION

Magnetic resonance imaging (MRI) is the "gold standard" in the characterization of tumors of the musculoskeletal system, on account of its high resolution, tissue contrast, and multiplanar capacity[1–6]. Additionally, MRI offers several advantages when compared with other imaging methods in

* Study developed at Clínicas de Diagnóstico Por Imagem (CDPI) and Multi-Imagem, Department of Radiology – Universidade Federal do Rio de Janeiro (UFRJ), and Instituto Nacional de Câncer (INCA), Rio de Janeiro, RJ, Brazil.

1. MD, Radiologist at Clínica de Diagnóstico Por Imagem (CDPI), Rio de Janeiro, RJ, Brazil.

2. MDs, Radiologists at Clínicas de Diagnóstico Por Imagem (CDPI) and Multi-Imagem, Rio de Janeiro, RJ, Brazil.

3. Physicist at Clínicas de Diagnóstico por Imagem (CDPI) and Multi-Imagem, Rio de Janeiro, RJ, Brazil.

4. MDs, Orthopedists at Instituto Nacional de Câncer (INCA), Rio de Janeiro, RJ, Brazil.

5. MD, Radiologist, Clinical Director, Clínicas de Diagnóstico por Imagem (CDPI) and Multi-Imagem, Rio de Janeiro, RJ, Brazil.

6. Post-Doctorate, Associate Professor of Radiology, Universidade Federal do Rio de Janeiro (UFRJ), MD, Radiologist at Clínicas de Diagnóstico por Imagem (CDPI) and Multi-Imagem, Rio de Janeiro, RJ, Brazil.

Mailing address: Dra. Flávia M. Costa. Avenida das Américas, 4666, sala 325, Barra da Tijuca. Rio de Janeiro, RJ, Brazil, 22631-004. E-mail: flávia26rio@hotmail.com

Received May 7, 2009. Accepted after revision June 29, 2009.

the evaluation and staging of bone and soft tissue tumors[3].

Several studies have already demonstrated morphological parameters as a criterion for differentiating benign from malignant musculoskeletal tumors, such as size, margins demarcation, involvement of adjacent vital structures, homogeneity in signal intensity, and measurements of relaxation time[7–11]. However, in several cases conventional MRI presents low specificity in the differential diagnosis of musculoskeletal tumors, as many of the lesions present nonspecific characteristics. Nevertheless, advanced MRI techniques, such as perfusion and proton spectroscopy, have been associated with conventional MRI, with the objective of improving the diagnostic accuracy of this imaging method, in particular in the assessment of the malignancy potential of a lesion[12–18].

Perfusion MRI has been frequently utilized in the study of musculoskeletal system tumors[15,18–23]. Previous studies have demonstrated that the first contrast passage in the dynamic study characterizes the tissue vascularization and perfusion in tumors[22,24–28]. Tissues with high vascularization and high capillary permeability tend to an early and intense contrast uptake as compared with less vascularized tissues[27]. With this technique, tumor-like lesions may be qualitatively evaluated by time to signal intensity curves (TIC – time intensity curves) and quantitatively by calculating the numerical value of the curve in percentage of signal increase per minute (slope – % per minute). However, an overlapping between the values of the perfusion curves (quantitative and qualitative) was demonstrated in highly vascularized benign lesions and in poorly vascularized malignant tumors[6,15,18,19,22]. For this reason, the combination of the qualitative pattern of the curves (TIC) and the quantitative value (slope in % per minute), associated with conventional MRI and proton spectroscopy, could be useful for narrowing the differential diagnosis of musculoskeletal tumors.

Proton spectroscopy is a noninvasive advanced MRI technique that is useful for evaluating musculoskeletal system tumors[12,14,29]. By means of this technique, one can detect malignancy markers such as increased choline peak, a component of cell membrane that reflects the high cell turnover, suggesting the malignancy potential of the lesions[30–32]. A previous study has demonstrated good results of spectroscopy in the differentiation between benign and malignant musculoskeletal tumors, with sensitivity, specificity and accuracy of respectively 95%, 82% and 89%[12]. However, the combination of this technique with perfusion and conventional MRI may further increase the MRI accuracy in the differential diagnosis of musculoskeletal tumors.

The present study was aimed at evaluating the role played by advanced MRI techniques, such as proton spectroscopy and perfusion, in the differential diagnosis of musculoskeletal system tumors.

MATERIALS AND METHODS

Patients

In the period between April, 2005 and January, 2007, 55 patients with musculoskeletal system tumors were studied (40 men and 15 women; mean age of 39 years, ranging between 20 days and 80 years). The patients had not undergone any surgical procedure or adjuvant treatment in the previous 10-year period. All the patients and/or family members signed a term of free and informed consent, and the study was approved by the Committee for Ethics in Research of the Institution.

Conventional MRI

All studies were performed in a 1.5 T Avanto® equipment (Siemens Medical Systems, Erlangen, Germany), with body coils or surface coils, depending upon the site and diameter of the lesion. The conventional protocol was performed, including coronal, sagittal and axial sections on weighted T1-fast spin echo (FSE) sequences (repetition time (TR)/echo time (TE): 426/15 ms; matrix: 521 × 512) and short inversion time recovery (STIR) (TR/TE: 3500/130 ms; inversion time (TI): 30 ms; matrix: 512 × 512) and T2-weighted FSE in the axial plane (TR/TE: 3600/104 ms; matrix: 512 × 512). Field of view (FOV), slice thickness and spacing between slices varied according with the tumor size.

Perfusion (dynamic contrast enhancement study) MRI

Dynamic contrast enhancement study was performed during intravenous bolus injection of 0.1 mmol/kg of gadolinium (Magnevist®; Schering AG, Berlin, Germany) with an infusion pump at a 2 ml/s flow rate, followed by 20 ml of saline solution. This study was performed with T1-weighted gradient echo sequence (TR/TE/TI: 606/1.34/300 ms; flip angle: 20°; matrix: 256 × 102), with a total of five sections with slice thickness and spacing between slices varying according with the tumor size. Total acquisition time was approximately five minutes and, at the end, T1-weighted FSE images were acquired with fat suppression in the axial and coronal planes (TR/TE: 759/10 ms; matrix: 512 × 512).

In order to evaluate perfusion data three regions of interest (ROI) of equal size were positioned in three different points: 1) within the lesion, in areas where there was intense early contrast uptake; 2) within an artery; 3) in the contralateral healthy muscle. All ROIs were positioned by an experienced radiologist specialized in musculoskeletal imaging. Based on the selected ROI, quantitative and qualitative analyses of the perfusion curves were performed with a standard software (mean curve) available in the workstation (Leonardo®; Siemens Medical Systems, Erlangen, Germany). Besides the qualitative evaluation of the TICs, the slope (% per minute) was calculated with the following formula:

$$\text{slope} = (SI_{max} - SI_{prior}) \times 100/(SI_{prior} \times T_{max})$$

where: SI_{prior} represents the values of the signal intensity before the intravenous gadolinium injection; SI_{max} is the value of signal intensity at T_{max}; and T_{max} indicates the time in which the relative value of signal intensity $SI\ (SI/SI_{prior})$ does not present an increase > 3% compared with the values at $T_{max.}$[15].

Two experienced radiologists specialized in musculoskeletal imaging, who did not have access to the histopathologic diagnosis of the lesions, classified the TICs patterns into the following types[16,18,20]: type I – absence of contrast uptake or minimum contrast uptake; type II – slow and gradual contrast uptake; type III – rapid and

early contrast uptake, followed by a plateau phase; type IV – rapid and early contrast uptake followed by a washout phase; type V – rapid and early contrast uptake followed by slow and sustained uptake.

Proton spectroscopy

Proton spectroscopy was performed with a single voxel with the point-resolved spectroscopy sequence and TE = 135 ms. The volumes of interest (ranging from 3.4 cm^3 to 8 cm^3) were positioned by two experienced radiologists, in the areas presenting early and intense contrast uptake, avoiding the inclusion of bone structures, fat and muscles. In patients presenting with tumor with subtle and slow contrast uptake or absence of uptake after the five minutes of the perfusion study, the voxel was positioned on areas presenting contrast uptake in the delayed images. Spectroscopy data were post-processed by means of a standard software (Spectroscopy®; Siemens, Erlangen, Germany). The presence of a choline peak within the lesion was defined by the 3.2 ppm peak on the spectral curve[12].

Histological data

The final diagnosis of the tumors was based on the results of histological evaluation, as shown on Table 1. Only the patients with lesions < than 4 cm and typical imaging findings of hemangioma (n = 2) and lipoma (n = 3), which did not present characteristics of malignancy and were stable after one-year follow-up, were not submitted to biopsy.

Statistical analysis

Statistical analysis was performed with the Statistical Package for Social Sciences (SPSS) 11.0 software (SPSS Inc.; Chicago, USA), and $p < 0.01$ values were considered as statistically significant. In order to evaluate the difference of the mean value of the quantitative analysis of the curve amongst the different groups, the Levene test was utilized to access the variables homogeneity, followed by the Student t test. The chi-squared test was utilized for categorical variables, and for the 2 × 2 tables, the Fischer's exact test was utilized.

RESULTS

Table 1 demonstrates histopathological findings, proton spectroscopy and qualitative and quantitative analyses of the perfusion curves of the 55 studied tumors (Figures 1 to 6).

Qualitative analysis – time-signal intensity curves (TIC*)*

Considering the TICs patterns, curves type I and II were found in 17 (85%) benign tumors and in only 3 (15%) malignant

Table 1 Summary of data regarding the 55 cases of musculoskeletal tumors.

Case	Age (years)	Sex	Location	Histological diagnosis	Malignant or benign	Type of TIC	Slope value (% per minute)	Choline peak	Tumor size (cm)
1	25	M	Arm	Synovial sarcoma	Malignant	IV	36%	Yes	17
2	68	M	Axillary region	Breast metastasis	Malignant	III	27%	No	4.3
3	25	M	Thigh	Hemangioma	Benign	II	8%	No	3
4	19	M	Thigh	Low-grade myxoid liposarcoma	Malignant	II	16%	No	13
5	33	F	Hip	Grade I chondrosarcoma	Malignant	III	18%	No	2.9
6	18	M	Thigh	Indifferentiated high-grade sarcoma	Malignant	IV	87%	Yes	8
7	54	M	Pelvis	Osteoblastic osteosarcoma	Malignant	IV	218%	Yes	23
8	59	M	Lumbar spine	Stomach matastasis	Malignant	IV	83%	Yes	6
9	62	M	Hip	Synovial sarcoma	Malignant	III	135%	Yes	20
10	19	F	Thigh	Hemangioma	Benign	II	11%	No	3.6
11	80	F	Thigh	Malignant fibrous histiocytoma	Malignant	IV	106%	Yes	15
12	13	F	Pelvis	Chodroblastic osteosarcoma	Malignant	III	81%	Yes	7.5
13	13	F	Thigh	High-grade sarcoma (spindle and ovoid cells)	Malignant	III	101%	Yes	9
14	25	M	Forearm	Low-grade mixofibrosarcoma	Malignant	II	11%	Yes	14
15	40	M	Thigh	Undifferentiated liposarcoma	Malignant	III	80%	Yes	8.2
16	40	M	Gluteus	Intermuscular lipoma	Benign	I	2%	No	10
17	39	M	Knee	Hemorrhagic bursitis	Benign	V	16%	No	8
18	64	M	Thigh	Hemangioma	Benign	I	1%	No	5
19	10	F	Thigh	Leiomiosarcoma (high grade)	Malignant	IV	153%	Yes	4.5
20	49	F	Pelvis	Primitive neuroectodermal tumor (PNET)	Malignant	IV	75%	Yes	18
21	13	F	Thigh	Lipoma	Benign	I	1%	No	5
22	46	M	Thorax	Synovial sarcoma	Malignant	IV	101%	Yes	15
23	30	M	Thigh	Fibrosarcoma (high grade)	Malignant	III	104%	Yes	18
24	49	F	Ankle	Benign schwannoma	Benign	II	21%	No	3.6
25	48	M	Shoulder	Lipoma	Benign	I	1%	No	6
26	51	M	Shoulder	Desmoid tumor	Benign	III	41%	Yes	9
27	20 days	M	Thigh	Highly calcified fibrous bone tumor	Benign	I	1%	No	14
28	54	M	Knee	Osteosarcoma	Malignant	IV	44%	Yes	12
29	25	M	Thigh	Synovial sarcoma	Malignant	IV	233%	Yes	6
30	8	M	Shoulder	Aneurysmal bone cyst	Benign	III	19%	No	8.9

(Table 1 continues)

Table 1 Summary of data regarding the 55 cases of musculoskeletal tumors.

Case	Age (years)	Sex	Location	Histological diagnosis	Malignant or benign	Type of TIC	Slope value (% per minute)	Choline peak	Tumor size (cm)
31	51	M	Shoulder	Bladder metastasis	Malignant	IV	156%	Yes	16
32	54	M	Arm	Malignant fibrous histiocytoma	Malignant	IV	181%	Yes	12
33	76	M	Thorax	Hematoma	Benign	I	7%	No	8
34	29	M	Wrist	Intraosseous ganglion cyst	Benign	I	0%	No	4
35	61	M	Pelvis	Leiomiosarcoma (grade III)	Malignant	IV	260%	Yes	12
36	69	M	Arm	Pleomorphic sarcoma (high grade)	Malignant	IV	116%	Yes	11
37	42	M	Thigh	Hematoma	Benign	I	1%	No	7
38	29	M	Leg	Synovial sarcoma	Malignant	IV	175%	Yes	9
39	20	M	Shoulder	Aneurysmal bone cyst	Benign	III	60%	No	14
40	59	F	Knee	Desmoid tumor	Benign	II	8%	No	6
41	55	M	Knee	Intraosseous ganglion cyst	Benign	II	11%	No	5
42	55	M	Thorax	Benign fibrous histiocytoma	Benign	II	7%	No	7
43	57	M	Foot	Leiomyoma	Benign	II	14%	No	10
44	31	M	Thorax	Intramuscular abscess	Benign	III	31%	Yes	16
45	17	F	Arm	Myositis ossificans	Benign	III	20%	No	10
46	50	F	Thigh	Hemangioma	Benign	III	60%	No	5
47	11	M	Thorax	Fibrous dysplasia	Benign	II	31%	No	6
48	5	M	Arm	Lipoblastoma	Benign	III	59%	No	13
49	15	M	Knee	Osteoblastic osteosarcoma	Malignant	IV	131%	Yes	10
50	29	F	Gluteus	Hemangioma	Benign	III	84%	No	6.4
51	56	F	Gluteus	Osteoblastic osteosarcoma	Malignant	IV	58%	Yes	7.8
52	36	F	Thigh	Malignant schwannoma	Malignant	II	12%	Yes	13.5
53	30	M	Pelvis	Giant cell tumor	Benign	III	111%	No	5.6
54	29	M	Thigh	Chronic calcified hematoma	Benign	II	8%	No	12.5
55	57	M	Knee	Aneurysmal bone cyst	Benign	IV	147%	No	5.4

M, male; F, female.

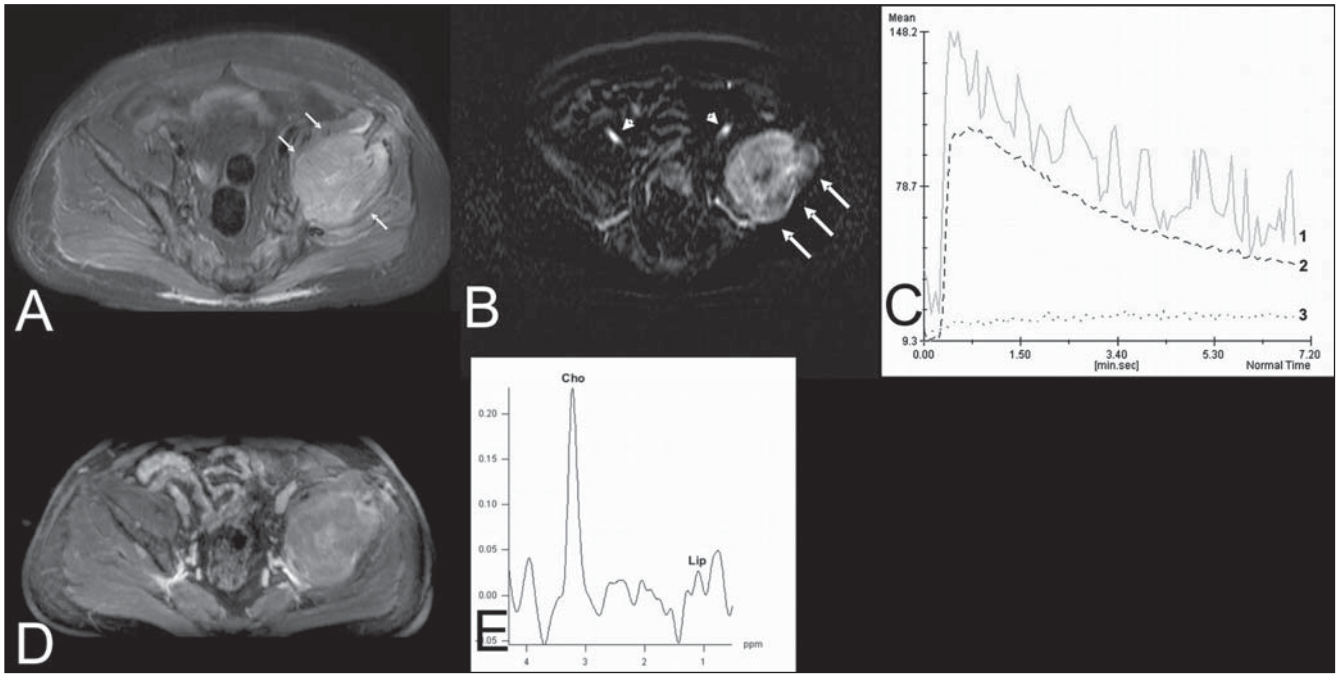

Figure 1. *Case 35.* Grade III leiomyosarcoma. **A:** Axial, STIR image showing extensive ovoid lesion with hyperintense signal (arrows) in the left iliac bone. **B:** Image submitted to the technique subtraction in the axial plane of the arterial phase of the dynamic contrast-enhancement study demonstrating the contrast uptake by the tumor (arrows), external iliac arteries (arrowheads) and the healthy muscle. **C:** The artery (1) and tumor (2) TIC patterns correspond to type IV and that of the healthy muscle (3) corresponds to type I. The slope value of the tumor curve is 260%/minute. **D:** The tumor presents homogeneous contrast uptake demonstrated on the T1-weighted sequence with fat suppression in the axial plane after intravenous gadolinium injection and dynamic study. **E:** The spectral analysis shows the choline peak (Cho) at 3.2 ppm, suggesting malignancy potential.

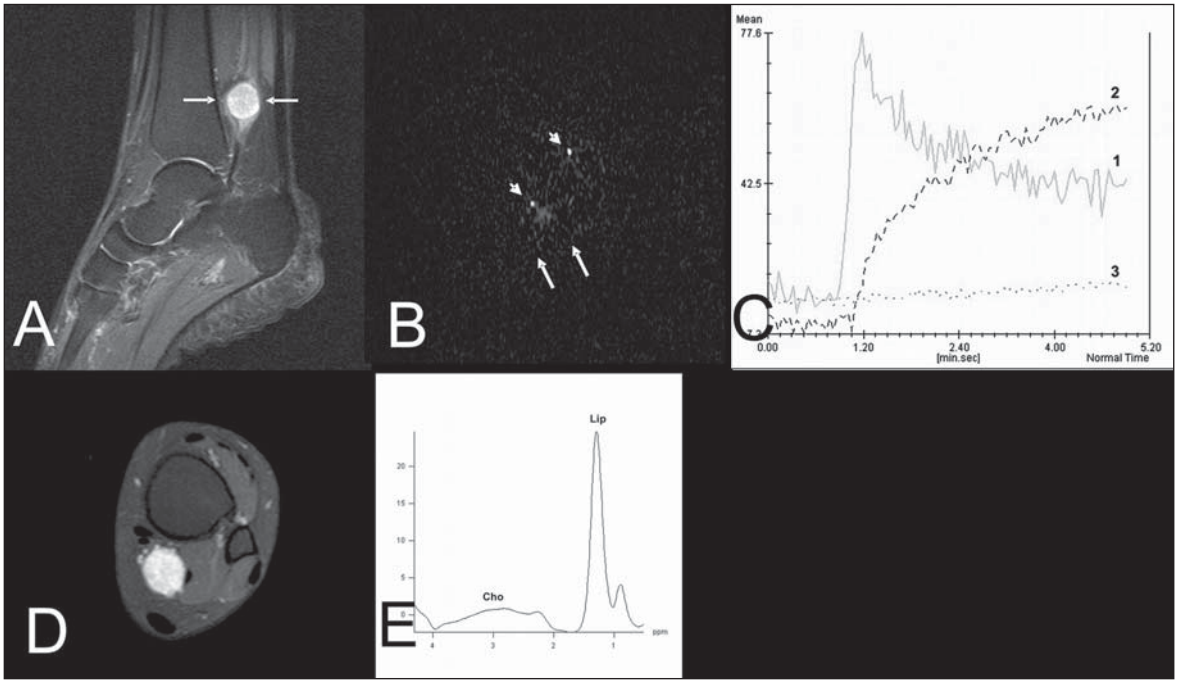

Figure 2. *Case 24.* Benign schwannoma. **A:** Sagittal, STIR image showing an ovoid, solid, well defined hyperintense lesion (arrows), in the tarsal tunnel. **B:** Image submitted to the subtraction technique in the axial plane in the arterial phase of the contrast dynamic study showing the contrast uptake by the arteries (arrowheads), but not by the tumor (arrows). **C:** The artery TIC pattern (1) is of type IV, the tumor's (2) is of type II and the healthy muscle's (3) is of type I. The slope value of the tumor is 21%/minute. **D:** The tumor presents homogeneous contrast uptake in the delayed phase, identified only on axial T1-weighted images with fat suppression. **E:** The spectral analysis did not demonstrate choline peak (Cho) at 3.2 ppm.

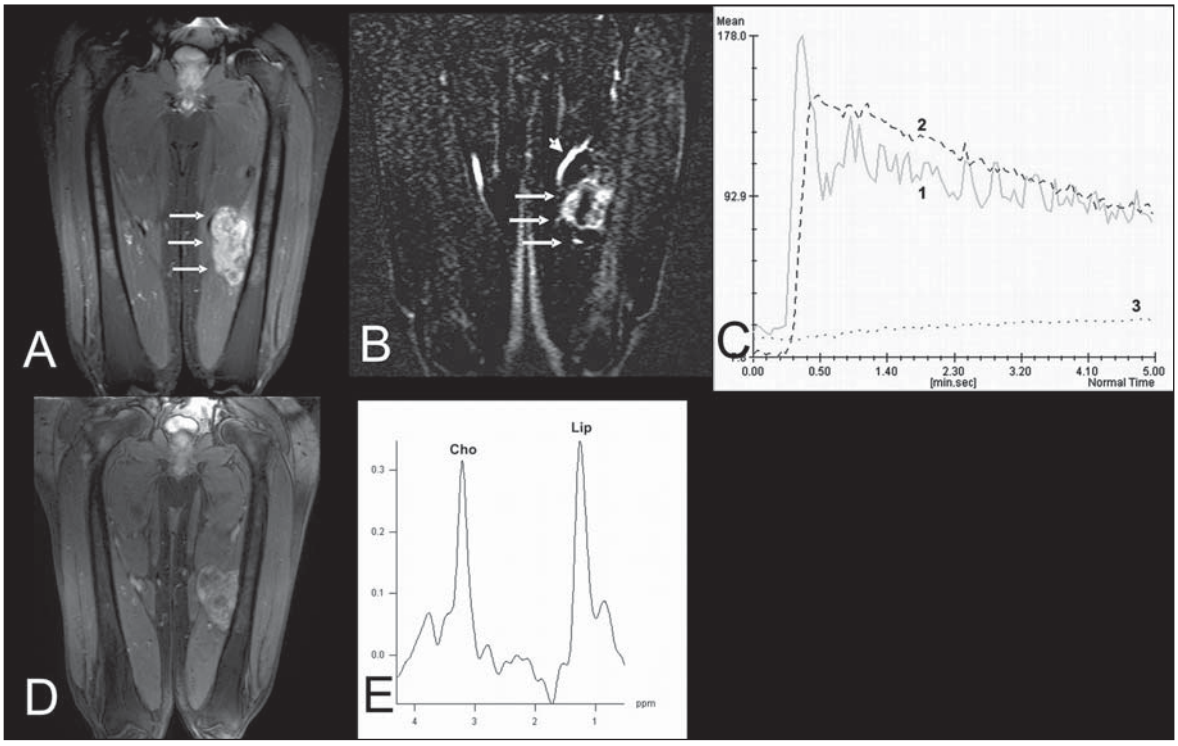

Figure 3. *Case 6.* High grade undifferentiated sarcoma. **A:** Coronal, STIR image shows a large, well defined, hyperintense lesion with an elongated aspect (arrows), intermingled with the adductor and vastus medialis muscles at left. **B:** Image submitted to the subtraction technique in the coronal plane, in the arterial phase of the dynamic contrast enhancement study, demonstrating the contrast uptake by the tumor (arrows), by the superficial femoral artery (arrowhead) and absence of uptake by the muscle. **C:** The TIC patterns of the artery (1) and of the tumor (2) are of the type IV and the healthy muscle TIC (3) is type I. The slope value of the tumor is 87%/minute. **D:** The tumor shows homogeneous contrast uptake on delayed. images of the T1-weighted sequence with fat suppression in the axial plane. **E:** The spectral analysis shows choline peak (Cho) at 3.2 ppm.

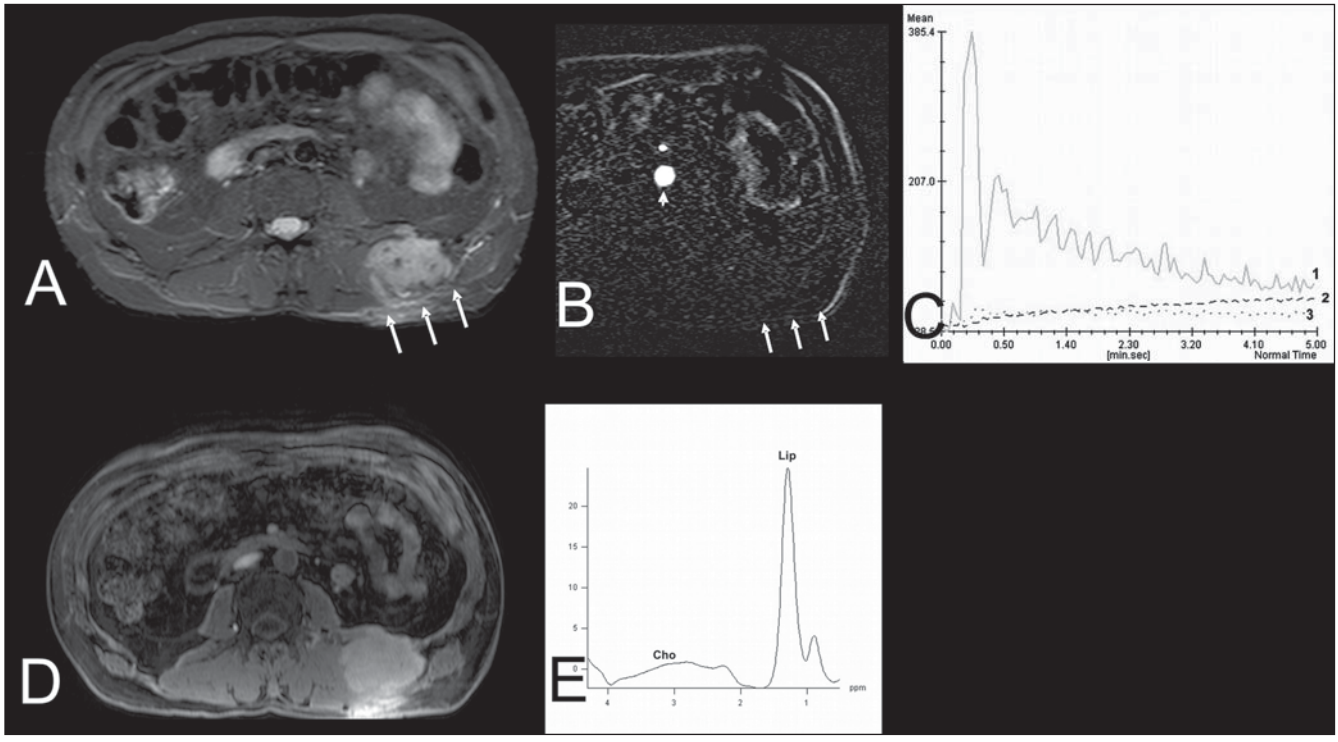

Figure 4. *Case 42.* Benign fibrous histiocytoma. **A:** Axial, STIR image showing expansile hyperintense ovoid, well defined lesion in the soft parts of the dorsolumbar transition at left (arrows). **B:** Arterial phase of the dynamic contrast enhancement study in the axial plane, submitted to the subtraction technique, showing the contrast within the arteries (arrowheads) and absence of contrast within the tumor (arrows). **C:** The TIC pattern of the artery (1) is of type IV, and the tumor's (2) and healthy muscle's are type I. The slope value of the tumor is 7%/minute. **D:** The tumor presented late contrast uptake, seen on the T1-weighted images with fat suppression in the axial plane. **E:** The spectral analysis did not demonstrate choline peak (Cho) at 3.2 ppm.

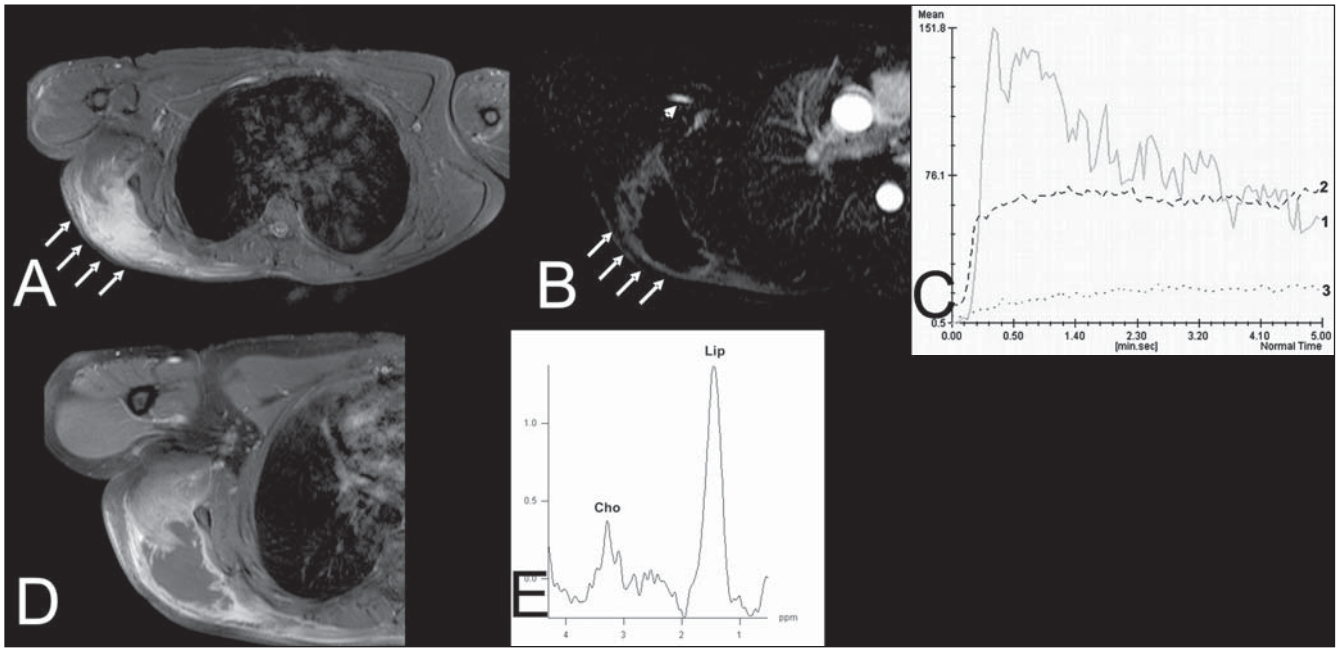

Figure 5. *Case 44.* Intramuscular abscess. **A:** Axial, STIR image showing elongated, expansile lesion with partially defined limits, heterogeneous signal intensity, remarkably hyperintense (arrows), in the muscular planes of the right scapular region. **B:** Arterial phase of the dynamic contrast enhancement study in the axial plane, submitted to the subtraction technique, showing contrast in the arteries (arrowheads) and uptake in the tumor peripheral region (arrows). **C:** The TIC pattern of the artery (1) is of the type IV, the tumor's (2) is of type III and healthy muscle's (3) is of type I. The slope value of the lesion is 31%/minute. **D:** The lesion presents peripheral contrast uptake, with the necrotic center visualized on delayed T1-weighted images with fat suppression in the axial plane. **E:** The spectral analysis shows a choline peak (Cho) at 3.2 ppm.

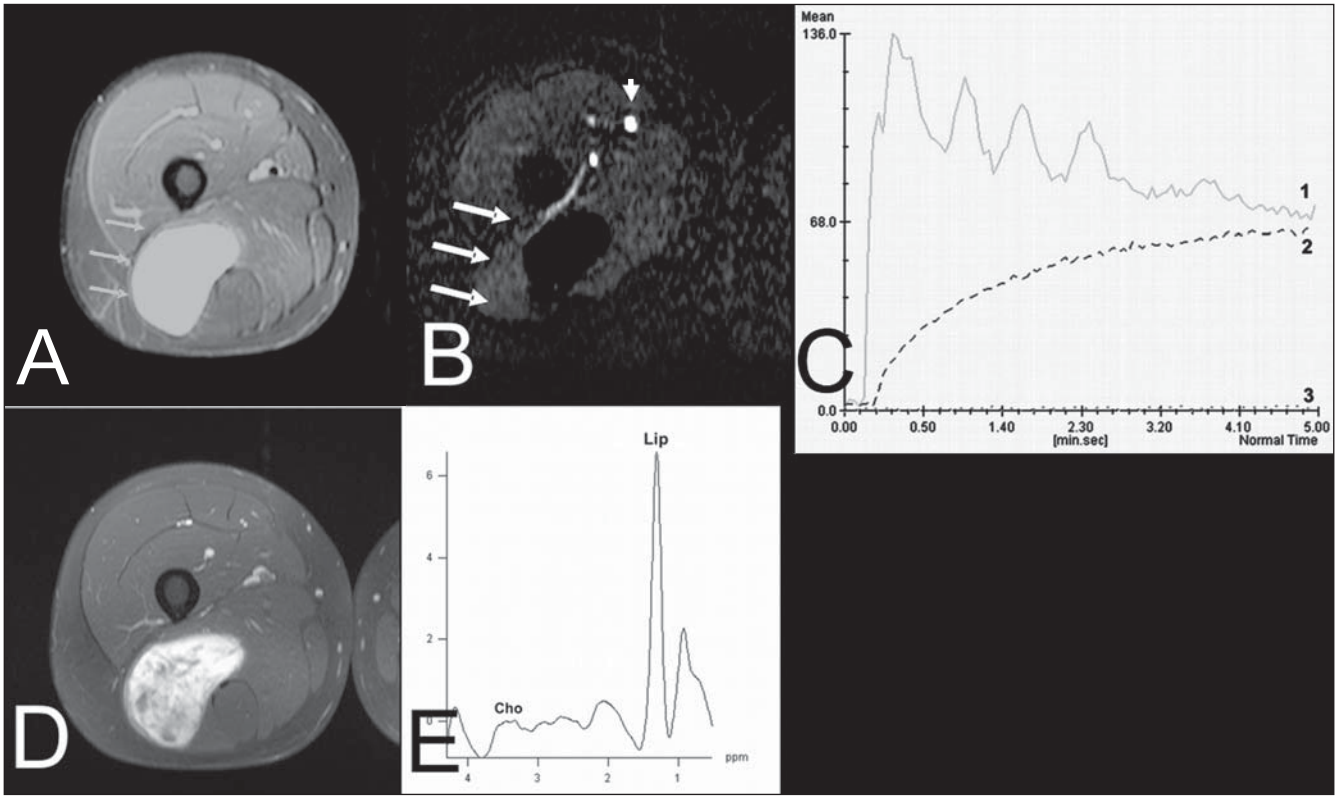

Figure 6. *Case 4.* Low-grade myxoid liposarcoma. **A:** Coronal, STIR sequence shows extensive, hyperintense, elongated, well defined lesion (arrows) in the posterior region of the right thigh. **B:** Arterial phase of the dynamic contrast enhancement study, submitted to the subtraction technique in the axial plane, showing contrast within the femoral arteries (arrowhead), absence of contrast within the tumor (arrows) and in the healthy muscle. **C:** The TIC pattern of the artery (1) is of type IV, the tumor's (2) is of type II and the healthy muscle (3) is of type I. The slope value of the tumor is 16%/minute. **D:** The tumor demonstrates homogeneous contrast uptake at the delayed phase, visualized on the T1-weighted sequence with fat suppression in the axial plane. **E:** The spectral analysis did not demonstrate choline peak (Cho) at 3.2 ppm.

tumors (low-grade myxoid liposarcoma, low-grade myxofibrosarcoma and malignant schwannoma). The type IV curve was found in 17 (89.5%) malignant tumors and in only one benign tumor (aneurismal bone cyst). The type V curve was found in only one benign lesion (hemorrhagic prepatellar bursitis). The type III curve was found in nine (56.2%) benign tumors and in seven (43.8) malignant tumors. There was a strong relation between curves of types I and II and benign tumors, and between type IV curves and malignant tumors ($p < 0.0001$).

Quantitative analysis – slope values

There was a significant difference of the slope values of benign lesions (mean, 27.5% per minute; ranging from 0–147%) in relation to malignant lesions (mean, 110.9% per minute; ranging from 11–260%) ($p < 0.0001$). Although an overlapping between the slope values of some benign and malignant lesions was found, the best cutoff value for the differentiation of these lesions was 39.9%/minute, with sensitivity, specificity, accuracy, positive and negative predictive values of 81%, 75%, 78%, 76% and 81% respectively.

Proton spectroscopy

The presence of choline peak (3.2 ppm) was demonstrated in 26 (47.3%) of the 55 cases of musculoskeletal tumors. In 24 of the 27 (88.9%) patients with malignant tumors, choline peaks were demonstrated. The three cases which did not present the peak were the following: one breast metastasis recurrence after 20 years, one grade I intraosseous chondrosarcoma and one low-grade myxoid liposarcoma. Of the 28 benign lesions, only 2 (7.1%) demonstrated choline peaks (one intramuscular abscess and one desmoid tumor). There was a statistically significant difference in the differentiation between benign and malignant tumors evaluated by proton spectroscopy ($p < 0.0001$). The choline peak accuracy was of 91%, specificity was 92%, sensitivity was 87.5%, negative predictive value was 88.5% and positive predictive value was 92%.

DISCUSSION

Proton spectroscopy of musculoskeletal tumors has been described in other studies[12,14,29]. Wang et al.[12] have analyzed the presence of choline peaks in 36 patients with soft parts and bone tumors. These authors have found 89% accuracy of this technique in the differentiation between benign and malignant lesions. Fayad et al.[29] have evaluated histopathological specimens from 13 musculoskeletal tumors with proton spectroscopy and demonstrated choline peaks significantly higher in areas of histologically confirmed malignant tumors. In the present study, the accuracy of the presence of choline peaks detected by proton spectroscopy for differentiation between malignant and benign musculoskeletal tumors was 91%. In this

casuistic three false negative results were found: one case of late recurrence from a breast tumor metastasis, one hypocellular myxoid liposarcoma, according to histopathological analysis, and a grade I intraosseous chondrosarcoma (< 3.0 cm). Wang et al.[12] have suggested that the small amount of available protons in the tissue, associated with the effects of magnetic susceptibility found in the bone, may contribute for a false negative result in the choline detection. Considering the two false positive results (one intramuscular abscess and one hypercellular desmoids tumor), previous studies[12,30] have demonstrated that hypercellular benign tumors and inflammatory cells may demonstrate choline peaks at spectral analysis without presenting malignant cells[12,30,32–34].

Previous researches have utilized, albeit with some limitations, dynamic contrast enhancement study (perfusion) to differentiate benign from malignant musculoskeletal tumors[22,35]. The slope values obtained in the dynamic study provides information on tissue vascularization and perfusion in a lesion. This variable may be related with the malignancy potential of the tumors, although there is some overlapping between the values from benign and malignant tumors[19]. In the present study, slope values < 39.9% per minute were demonstrated preferably in benign tumors, while slope values > 39.9% per minute were mostly observed in malignant tumors. In some cases in the present study, results demonstrated high slope values in quite avascular benign tumors, a finding already described in previous studies[19,22]. As previously described, malignant tumors with low slope values were generally lesions with a low malignancy degrees, recurrences and necrotic tumors[15,16].

Considering soft tissue tumors, van Rijswijk et al.[18] have described intense and early contrast uptake followed by a plateau or washout phase (TIC types III and IV) as suggestive of malignancy. Van der Woude et al.[22] have differentiated soft tissue tumors between malignant and benign ones by utilizing the different TIC patterns, with 86%sensitivity and 81% specificity. On the other hand, bone tumors could not be differentiated by the same method. In the present series, the majority of malignant soft tissue and bone tumors demonstrated TIC curves of type IV with washout, which is present in highly vascularized lesions with small interstitial spacing[20]. Only one benign lesion (highly vascularized aneurysmal bone cyst) presented a TIC of type IV. TICs of types I and II were found in most of the benign lesions. Only three malignant tumors presented type II TIC: one low grade myxoid liposarcoma, one low grade myxofibrosarcoma, hypocellular and hypovascular at histopathological study, and one malignant schwannoma with extensive necrosis. In this study, type III TIC was not useful in differentiating benign from malignant tumors.

Considering the dynamic contrast enhancement study (perfusion) in association with proton spectroscopy, one observed that 23 of the 27 patients with malignant tumors presented slope values > 39.9% associated with the detection of choline peaks. By analyzing the benign tumors, only one of the 28 patients obtained the same result (desmoid tumor). Sensitivity, specificity and positive and negative predictive values of the association of both techniques were 85.1%, 96.4%, 95.8% and 87%, respectively. On the other hand, 17 of the 27 patients with malignant tumors obtained TIC type IV and detected choline peak, while no benign tumor presented the same result. The sensitivity, specificity and positive and negative predictive values were, respectively, 62.9%, 100%, 100% and 73%.

Finally, perfusion MRI (TIC and slope values) associated with proton spectroscopy (choline peak detection) may be useful in the differentiation of benign from malignant musculoskeletal tumors. The presences of type IV TIC, slope > 39.9% per minute and choline peak detection are highly suggestive of malignancy. Besides the diagnostic role, such techniques may also contribute in the planning of biopsy sites, as they indicate areas of viable tumor, allowing higher accuracy in the histopathological diagnosis, and facilitating the therapy planning.

Further studies with larger casuistics should confirm the importance of advanced MRI in the differential diagnosis of musculoskeletal tumors.

REFERENCES

1. Ma LD, Frassica FJ, McCarthy EF, et al. Benign and malignant musculoskeletal masses: MR imaging differentiation with rim-to-center differential enhancement ratios. Radiology. 1997;202: 739–44.
2. Blacksin MF, Ha DH, Hameed M, et al. Superficial soft-tissue masses of the extremities. Radiographics. 2006;26:1289–304.
3. Catalan J, Fonte AC, Lusa JRB, et al. Tumor de células gigantes ósseo: aspectos clínicos e radiográficos de 115 casos. Radiol Bras. 2006;39:119–22.
4. Gomes ACN, Silveira CRS, Paiva RGS, et al. Condrossarcoma em paciente com osteocondromatose múltipla: relato de caso e revisão da literatura. Radiol Bras. 2006;39:449–51.
5. Kransdorf MJ, Jelinek JS, Moser RP Jr, et al. Soft-tissue masses: diagnosis using MR imaging. AJR Am J Roentgenol. 1989;153:541–7.
6. Öztekin O, Argin M, Oktay A, et al. Intraosseous lipoma: radiological findings. Radiol Bras. 2008; 41:81–6.
7. Berquist TH, Ehman RL, King BF, et al. Value of MR imaging in differentiating benign from malignant soft-tissue masses: study of 95 lesions. AJR Am J Roentgenol. 1990;155:1251–5.
8. Totty WG, Murphy WA, Lee JK. Soft-tissue tumors: MR imaging. Radiology. 1986;160:135–41.
9. Crim JR, Seeger LL, Yao L, et al. Diagnosis of soft-tissue masses with MR imaging: can benign masses be differentiated from malignant ones? Radiology. 1992;185:581–6.
10. Sundaram M, McGuire MH, Schajowicz F. Soft-tissue masses: histologic basis for decreased signal (short T2) on T2-weighted MR images. AJR Am J Roentgenol. 1987;148:1247–50.
11. Moulton JS, Blebea JS, Dunco DM, et al. MR imaging of soft-tissue masses: diagnostic efficacy and value of distinguishing between benign and malignant lesions. AJR Am J Roentgenol. 1995; 164:1191–9.
12. Wang CK, Li CW, Hsieh TJ, et al. Characterization of bone and soft-tissue tumors with in vivo 1H MR spectroscopy: initial results. Radiology. 2004;232:599–605.
13. Geirnaerdt MJA, Hogendoorn PCW, Bloem JL, et al. Cartilaginous tumors: fast contrast-enhanced MR imaging. Radiology. 2000;214:539–46.
14. Fayad LM, Barker PB, Jacobs MA, et al. Characterization of musculoskeletal lesions on 3-T proton MR spectroscopy. AJR Am J Roentgenol. 2007;188:1513–20.
15. Erlemann R, Reiser MF, Peters PE, et al. Musculoskeletal neoplasms: static and dynamic Gd-DTPA-enhanced MR imaging. Radiology. 1989;171:767–73.
16. Van Herendael BH, Heyman SRG, Vanhoenacker FM, et al. The value of magnetic resonance imaging in the differentiation between malignant peripheral nerve-sheath tumors and non-neurogenic malignant soft-tissue tumors. Skeletal Radiol. 2006;35:745–53.
17. Shapeero LG, Vanel D, Verstraete KL, et al. Dynamic contrast-enhanced MR imaging for soft tissue sarcomas. Semin Musculoskelet Radiol. 1999;3:101–14.
18. van Rijswijk CSP, Geirnaerdt MJA, Hogendoorn PCW, et al. Soft-tissue tumors: value of static and

dynamic gadopentetate dimeglumine-enhanced MR imaging in prediction of malignancy. Radiology. 2004;233:493–502.

19. Verstraete KL, De Deene Y, Roels H, et al. Benign and malignant musculoskeletal lesions: dynamic contrast-enhanced MR imaging – parametric "first-pass" images depict tissue vascularization and perfusion. Radiology. 1994;192:835–43.
20. Tokuda O, Hayashi N, Taguchi K, et al. Dynamic contrast-enhanced perfusion MR imaging of diseased vertebrae: analysis of three parameters and the distribution of the time-intensity curve patterns. Skeletal Radiol. 2005;34:632–8.
21. Kajihara M, Sugawara Y, Sakayama K, et al. Evaluation of tumor blood flow in musculoskeletal lesions: dynamic contrast-enhanced MR imaging and its possibility when monitoring the response to preoperative chemotherapy – work in progress. Radiat Med. 2007;25:94–105.
22. van der Woude HJ, Verstraete KL, Hogendoorn PC, et al. Musculoskeletal tumors: does fast dynamic contrast-enhanced subtraction MR imaging contribute to the characterization? Radiology. 1998;208:821–8.
23. Fletcher BD, Hanna SL, Fairclough DL, et al. Pediatric musculoskeletal tumors: use of dynamic, contrast-enhanced MR imaging to monitor response to chemotherapy. Radiology. 1992; 184:243–8.
24. Verstraete KL, van der Woude HJ, Hogendoorn PCW, et al. Dynamic contrast-enhanced MR imaging of musculoskeletal tumors: basic principles and clinical applications. J Magn Reson Imaging. 1996;6:311–21.
25. Verstraete KL, Dierick A, De Deene Y, et al. First-pass images of musculoskeletal lesions: a new and useful diagnostic application of dynamic contrast-enhanced MRI. Magn Reson Imaging. 1994;12:687–702.
26. Fletcher BD, Hanna SL. Musculoskeletal neoplasms: dynamic Gd-DTPA-enhanced MR imaging. Radiology. 1990;177:287–8.
27. Verstraete KL, Vanzieleghem B, De Deene Y, et al. Static, dynamic and first-pass MR imaging of musculoskeletal lesions using gadodiamide injection. Acta Radiol. 1995;36:27–36.
28. Daldrup H, Shames DM, Wendland M, et al. Correlation of dynamic contrast-enhanced MR imaging with histologic tumor grade: comparison of macromolecular and small-molecular contrast media. AJR Am J Roentgenol. 1998;171:941–9.
29. Fayad LM, Bluemke DA, McCarthy EF, et al. Musculoskeletal tumors: use of proton MR spectroscopic imaging for characterization. J Magn Reson Imaging. 2006;23:23–8.
30. Maheshwari SR, Mukherji SK, Neelon B, et al. The choline/creatine ratio in five benign neoplasms: comparison with squamous cell carcinoma by use of in vitro MR spectroscopy. AJNR Am J Neuroradiol. 2000;21:1930–5.
31. Bartella L, Morris EA, Dershaw DD, et al. Proton MR spectroscopy with choline peak as malignancy marker improves positive predictive value for breast cancer diagnosis: preliminary study. Radiology. 2006;239:686–92.
32. Rand SD, Prost R, Haughton V, et al. Accuracy of single-voxel proton MR spectroscopy in distinguishing neoplastic from nonneoplastic brain lesions. AJNR Am J Neuroradiol. 1997;18:1695–704.
33. Bitsch A, Bruhn H, Vougioukas V, et al. Inflammatory CNS demyelination: histopathologic correlation with in vivo quantitative proton MR spectroscopy. AJNR Am J Neuroradiol. 1999;20: 1619–27.
34. Krouwer HG, Kim TA, Rand SD, et al. Single-voxel proton MR spectroscopy of nonneoplastic brain lesions suggestive of a neoplasm. AJNR Am J Neuroradiol. 1998;19:1695–703.
35. Hsieh TJ, Li CW, Chuang HY, et al. Longitudinally monitoring chemotherapy effect of malignant musculoskeletal tumors with in vivo proton magnetic resonance spectroscopy: an initial experience. J Comput Assist Tomogr. 2008;32:987–94.